- Molecular Ionics in Supramolecular Assemblies with Channel Structures Containing Lithium Ions
  Moriya,M.; Kitaguchi, H.; Nishibori, E.; Sawa, H.; Sakamoto, W.; Yogo, T. *Chem. Eur. J.* **2012**, *18*, 15305–15309.
  Abstract:

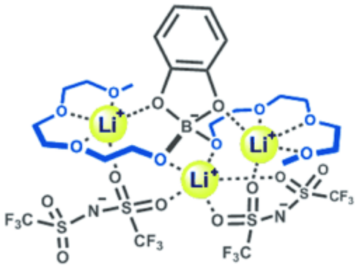

A novel trilithium compound, $Li_3[B(C_6H_4O_2)\{O(CH_2CH_2O)_3CH_3\}_2][N(SO_2CF_3)_2]_2$ (**1**-2.0), with solid-state ionic conductivity was synthesized. The crystal structure of **1**-2.0 consists of the one-dimensional ionic conduction paths. The paths were afforded as a result of the self-assembled stacking of the component molecules of **1**-2.0 with channel structures containing lithium ions. In this supramolecule, one lithium ion holds the component molecules in specific positions to construct a supramolecular structure with thermally stable ionic conduction paths and the others behave as carrier ions exhibiting selective lithium-ion conductivity. Owing to the existence of both roles for the lithium ions, this electrolyte shows selective lithium-ion conductivity.

- Narcissistic versus Social Self-Sorting of Oligophenyleneethynylene Derivatives: From Isodesmic Self-Assembly to Cooperative Co-Assembly
  Mayoral, M. J.; Rest, C.; Schellheimer, J.; Stepanenko, V.; Fernández, G. *Chem. Eur. J.* **2012**, *18*, 15607–15611.
  Abstract:

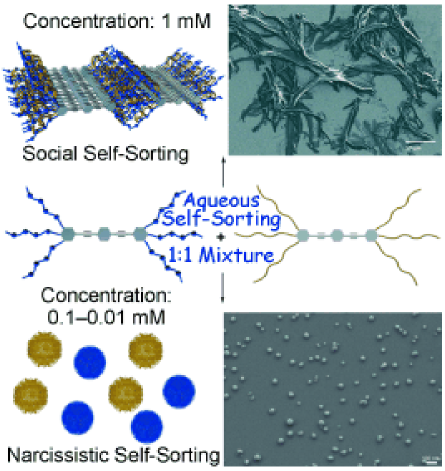

Narcissistic versus social! The self-assembly of two structurally related oligophenyleneethynylene derivatives featuring polar or nonpolar peripheral chains is reported. Their remarkable narcissistic versus social self-sorting behaviour in aqueous media can be controlled by concentration and solvent changes.

- Copper, BDNF and Its N-terminal Domain: Inorganic Features and Biological Perspectives
  Travaglia, A.; La Mendola, D.; Magrì, A.; Nicoletti, V. G.; Pietropaolo, A.; Rizzarelli, E. *Chem. Eur. J.* **2012**, *18*, 15618–15631.

Abstract:

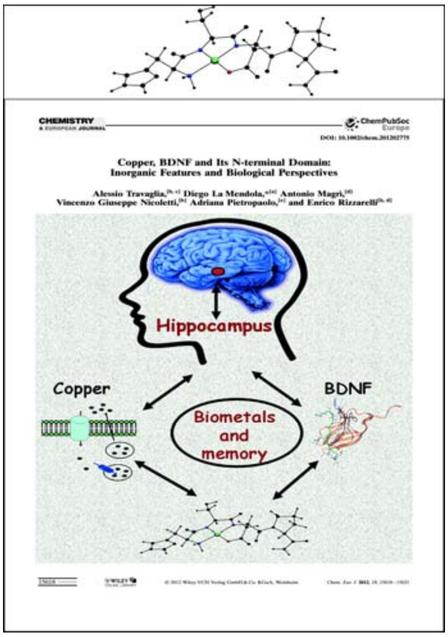

CHEMISTRY
A EUROPEAN JOURNAL

ChemPubSoc Europe

Copper, BDNF and Its N-terminal Domain:
Inorganic Features and Biological Perspectives

Alessio Travaglia, Diego La Mendola, Antonio Magrì,
Vincenzo Giuseppe Nicoletti, Adriana Pietropaolo, and Enrico Rizzarelli

Key complex: Brain-derived neurotrophic factor (BDNF) N-terminal domain binds copper(II) with the involvement of His-1 α-amino group and Asp-3 carboxylate. The peptide encompassing the sequence 1–12 of the amino-terminal domain (BDNF(1–12)) of human BDNF is able to bind Cu^{2+}. The predominant Cu^{2+}complex species, at physiological pH, is the $[CuH_{-2}L]^{2-}$ in which the metal ion is bound to an amino group, two amide nitrogen atoms, and a carboxylate group (NH_2, $2N^-$, COO^-_{Asp}) in a planar environment.

- Hard Autonomous Self-Healing Supramolecular Materials—A Contradiction in Terms?
  Hoogenboom, R. *Angew. Chem. Int. Ed.* **2012**, *51*, 11942-11944.
  Abstract:

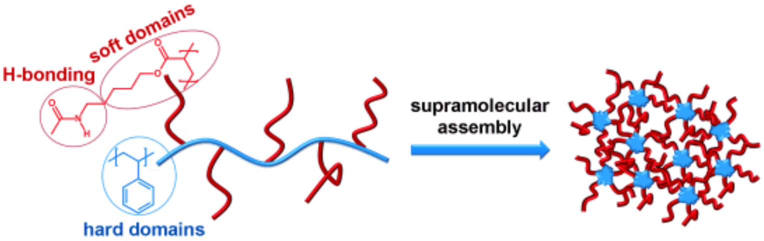

Achieving the unachievable: Hard supramolecular materials displaying autonomous self-healing have been considered unachievable because of the mobility required to reconstitute supramolecular interactions after rupture. Now, relatively hard thermoplastic elastomers have been reported that meet these requirements. The picture shows a triblock copolymer containing soft supramolecular "self-healing" domains and hard, structure-giving domains.

- Template Assembly of Spin Crossover One-Dimensional Nanowires
  Martinho, P. N.; Lemma, T.; Gildea, B.; Picardi, G.; Müller-Bunz, H.; Forster, R. J.; Keyes, T. E.; Redmond, G.; Morgan, G. G. *Angew. Chem. Int. Ed.* **2012**, *51*, 11995–11999.
  Abstract:

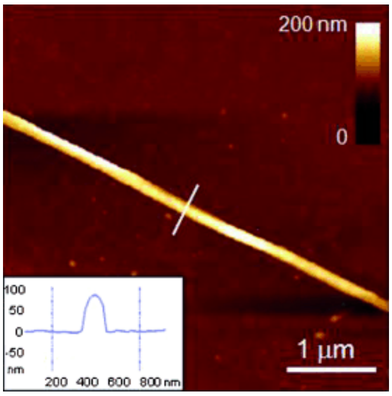

Wired for action: An alumina-based template method produces nanowires of an alkylated mononuclear spin-crossover FeIII complex. The wires can be isolated by dissolving the template in acid without decomposition of the product, and have a narrow distribution of diameter widths in the range of 80–100 nm. Electronic characterization of a single wire is possible by using Raman spectroscopy coupled to AFM (see picture).

- Unraveling Unidirectional Threading of α-Cyclodextrin in a [2]Rotaxane through Spin Labeling Approach
  Casati, C.; Franchi, P.; Pievo, R.; Mezzina, E.; Lucarini, M. *J. Am. Chem. Soc.* **2012**, *134*, 19108–19117.
  <u>Abstract:</u>

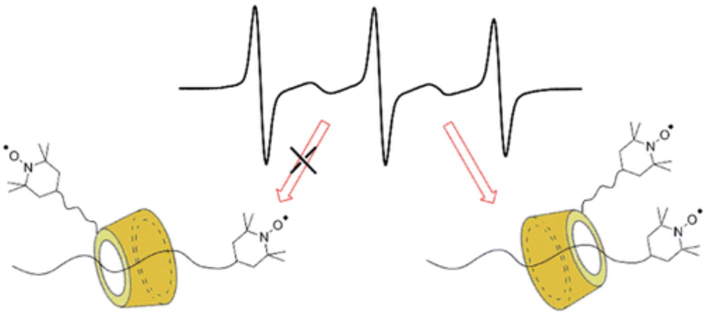

We present here the results of a CW-ESR investigation of a double spin labeled α-cyclodextrin-based [2]rotaxane that is characterized by the presence of nitroxide labels both at the wheel and at the dumbbell. This was accomplished by synthesizing a spin labeled α-CD (the wheel) that was mechanically blocked on a thread containing a nitroxide unit by a Cu(I) catalyzed azide–alkyne cycloaddition (CuAAC). Both ESI-MS analysis and NMR spectroscopy were used to provide evidence of the threading processes. Because of the unsymmetrical structure of both the wheel and the axle, two different geometrical isomers could be predicted on the basis of the orientation of the CD along the thread. By combining molecular dynamic calculations and information extracted from the CW-ESR spectra, we were able to determine the geometrical nature of the isomer that was isolated as the only species. The ESR spectra showed *J*-coupling between the two mechanically connected nitroxide units and were analyzed by a model assuming three main molecular states. The intramolecular noncovalent nature of spin exchange was confirmed by reversibly switching the magnetic interaction on–off by changing the pH of the solution in the presence of a competing macrocyclic host.

- Structural Parameters Governing the Dynamic Combinatorial Synthesis of Catenanes in Water

Cougnon, F. B. L.; Ponnuswamy, N.; Jenkins, N. A.; Pantoş, G. D.; Sanders, J. K. M. *J. Am. Chem. Soc.* **2012**, *134*, 19129–19135.

Abstract:

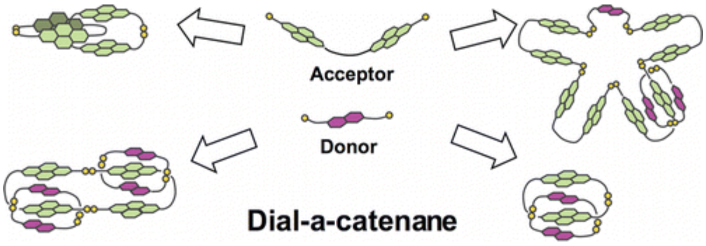

We report the first dynamic combinatorial synthesis in water of an all-acceptor [2]catenane and of different types of donor–acceptor [2] and [3]catenanes. Linking two electron-deficient motifs within one building block using a series of homologous alkyl chains provides efficient and selective access to a variety of catenanes and offers an unprecedented opportunity to explore the parameters that govern their synthesis in water. In this series, catenane assembly is controlled by a fine balance between kinetics and thermodynamics and subtle variations in the building block structure, such as the linker length and building block chirality. A remarkable and unexpected odd–even effect with respect to the number of atoms in the alkyl linker is reported.

- BODIPY-Based Ratiometric Fluorescent Sensor for Highly Selective Detection of Glutathione over Cysteine and Homocysteine
  Niu, L.-Y.; Guan, Y.-S.; Chen, Y-Z.; Wu, L.-Z.; Tung, C.-H.; Yang, Q.-Z. *J. Am. Chem. Soc.* **2012**, *134*, 18928–18931.
  Abstract:

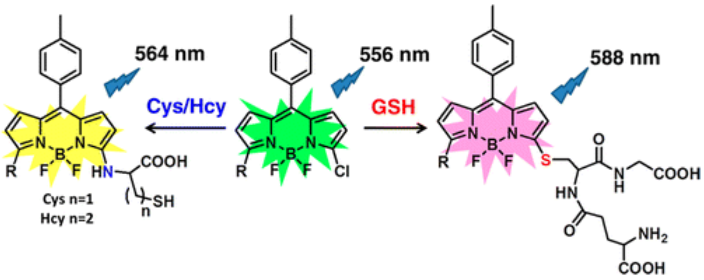

We report a ratiometric fluorescent sensor based on monochlorinated BODIPY for highly selective detection of glutathione (GSH) over cysteine (Cys)/homocysteine (Hcy). The chlorine of the monochlorinated BODIPY can be rapidly replaced by thiolates of biothiols through thiol–halogen nucleophilic substitution. The amino groups of Cys/Hcy but not GSH further replace the thiolate to form amino-substituted BODIPY. The significantly different photophysical properties of sulfur- and amino-substituted BODIPY enable the discrimination of GSH over Cys and Hcy. The sensor was applied for detection of GSH in living cells.

- Predicting Large CO_2 Adsorption in Aluminosilicate Zeolites for Postcombustion Carbon Dioxide Capture
  Kim, J.; Lin, L.-C.; Swisher, J. A.; Haranczyk, M.; Smit, B. *J. Am. Chem. Soc.* **2012**, *134*, 18940–18943.
  Abstract:

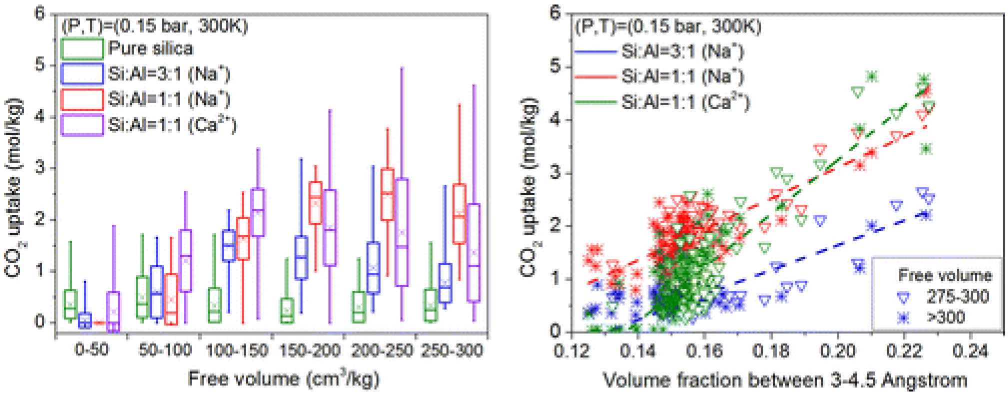

Large-scale simulations of aluminosilicate zeolites were conducted to identify structures that possess large CO_2 uptake for postcombustion carbon dioxide capture. In this study, we discovered that the aluminosilicate zeolite structures with the highest CO_2 uptake values have an idealized silica lattice with a large free volume and a framework topology that maximizes the regions with nearest-neighbor framework atom distances from 3 to 4.5 Å. These predictors extend well to different Si:Al ratios and for both Na^+ and Ca^{2+} cations, demonstrating their universal applicability in identifying the best-performing aluminosilicate zeolite structures.

- Bay-substituted perylene bisimide dye with an undistorted planar scaffold and outstanding solid state fluorescence properties
  Lin, M.-J.; Jiménez, Á. J. ; Burschka, C.; Würthner, F. *Chem. Commun.* **2012,** *48,* 12050–12052.
  Abstract:

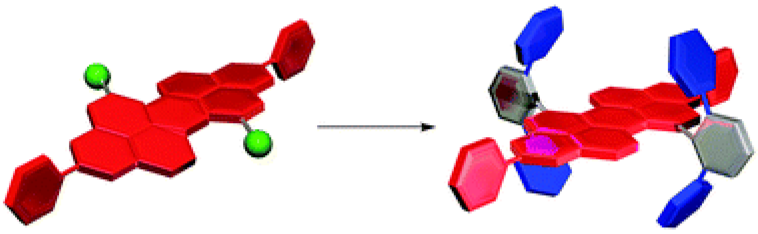

Single crystal X-ray analysis reveals a flat perylene π-scaffold for a perylene bisimide bearing bulky 2,6-diphenylphenoxy substituents at the 1,7 bay positions. The flat structure provides sharp vibronic progressions in the absorption and fluorescence spectra, the sterical shielding outstanding fluorescence quantum yields in the solid state.

- Cavity-containing, backbone-rigidified foldamers and macrocycles
  Yamato, K.; Kline, M.; Gong, B. *Chem. Commun.* **2012,** *48,* 12142–12158.
  Abstract:

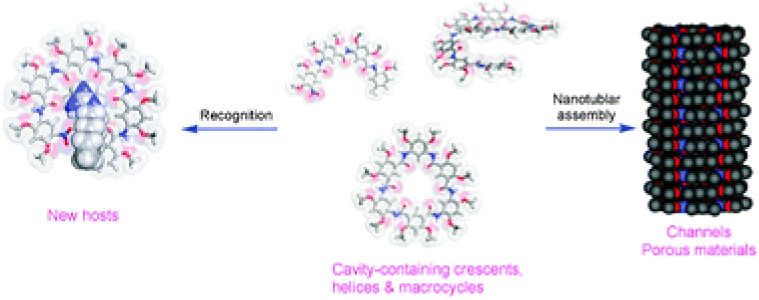

This Feature Article gives an account for a host of readily available foldamers and macrocycles with well-defined shapes and non-deformable cavities that appeared over the last decade. Efforts to create porous molecular structures have led to the establishment of an effective strategy for enforcing the folding of unnatural aromatic oligoamide strands based on an especially robust three-center (bifurcated) hydrogen-bonding interaction. Based on such a strategy, aromatic oligoamides adopting crescent and helical conformations that contain non-collapsible cavities of tunable diameters have been created. Extending the same folding principle to the preparation of aromatic polyamides that would adopt pore-containing helical conformation instead led to the discovery of a highly efficient, one-pot macrocyclization process. Such a one-pot macrocyclization process has been successfully applied to the preparation of macrocycles with aromatic amide, hydrazide, urea and other backbones. Mechanistic study indicates that the high efficiencies observed for the formation of these macrocycles are due to the folding of the corresponding uncyclized oligomeric precursors of the corresponding macrocycles. Oligoamide macrocycles, along with their uncyclized, cavity-containing counterparts, *i.e.*, crescent oligoamides, bind guests such as guanidinium (G) and octylguanidinium (OG) ions with tunable selectivity. Recent studies revealed that these rigid macrocycles tend to engage in extraordinarily strong, directional aggregation, leading to nanotubular assemblies containing pores of fixed sizes. Consistent with the presence of self-assembling nanopores, oligoamide macrocycles were found to assemble into transmembrane channels with high conductance.

- Dereplicating nonribosomal peptides using an informatic search algorithm for natural products (iSNAP) discovery
  Ibrahim, A.; Yang, L.; Johnston, C.; Liu, X.; Ma, B.; Magarvey, N. A. *Proc. Nat. Acad. Sci. USA* **2012**, *109*, 19196-19201.
  Abstract:

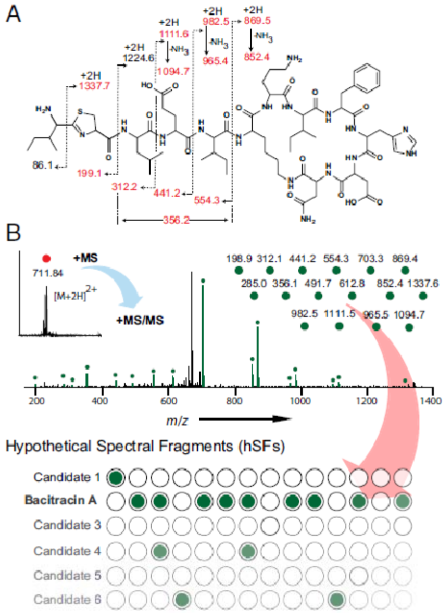

Nonribosomal peptides are highly sought after for their therapeutic applications. As with other natural products, dereplication of known compounds and focused discovery of new agents within this class are central concerns of modern natural product-based drug discovery. Development of a chemoinformatic library-based and informatic search strategy for natural products (iSNAP) has been constructed and applied to nonribosomal peptides and proved useful for true nontargeted dereplication across a spectrum of nonribosomal peptides and within natural product extracts.

- Counting primary loops in polymer gels
  Zhou, H.; Woo, J.; Cok, A. M.; Wang, M.; Olsen, B. D.; Johnson, J. A. *Proc. Nat. Acad. Sci. USA* **2012**, *109*, 19119-19124.
  Abstract:

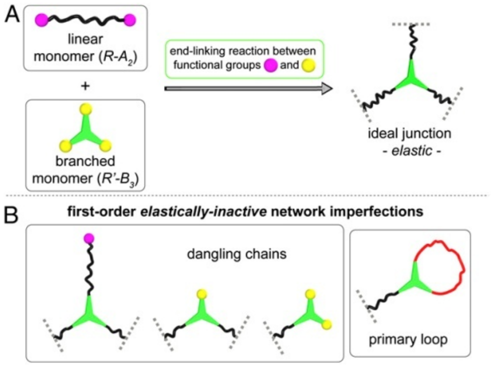

Much of our fundamental knowledge related to polymer networks is built on an assumption of ideal end-linked network structure. Real networks invariably possess topological imperfections that negatively affect mechanical properties; modifications of classical network theories have been developed to account for these defects. Despite decades of effort, there are no known experimental protocols for precise quantification of even the simplest topological network imperfections: primary loops. Here we present a simple conceptual framework that enables primary loop quantification in polymeric materials. We apply this framework to measure the fraction of primary loop junctions in trifunctional PEG-based hydrogels. We anticipate that the concepts described here will open new avenues of theoretical and experimental research related to polymer network structure.

- Broad-Spectrum Antimicrobial Supramolecular Assemblies with Distinctive Size and Shape
  Fukushima, K.; Tan, J. P. K.; Korevaar, P. A.; Yang, Y. Y.; Pitera, J.; Nelson, A.; Maune, H.; Coady, D. J.; Frommer, J. E.; Engler, A. C.; Huang, Y.; Xu, K.; Ji, Z.; Qiao, Y.; Fan, W.; Li, L.; Wiradharma, N.; Meijer, E. W.; Hedrick, J. L. *ACS Nano* **2012** *6*, 9191-9199.
  Abstract:

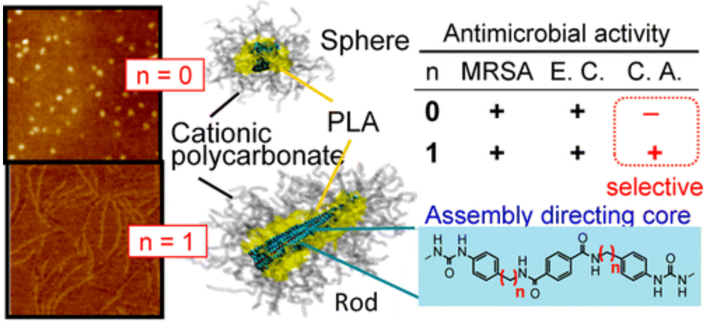

With the increased prevalence of antibiotic-resistant infections, there is an urgent need for innovative antimicrobial treatments. One such area being actively explored is the use of self-assembling cationic polymers. This relatively new class of materials was inspired by biologically pervasive cationic host defense peptides. The antimicrobial action of both the synthetic polymers and naturally occurring peptides is believed to be complemented by their three-dimensional structure. In an effort to evaluate shape effects on antimicrobial materials, triblock polymers were polymerized from an assembly directing terephthalamide-bisurea core. Simple changes to this core, such as the addition of a methylene spacer, served to direct self-assembly into distinct morphologies—spheres and rods. Computational modeling also demonstrated how subtle core changes could directly alter urea stacking motifs manifesting in unique multidirectional hydrogen-bond networks despite the vast majority of material consisting of poly(lactide) (interior block) and cationic polycarbonates (exterior block). Upon testing the spherical and rod-like morphologies for antimicrobial properties, it was found that both possessed broad-spectrum activity (Gram-negative and Gram-positive bacteria as well as fungi) with minimal hemolysis, although only the rod-like assemblies were effective against *Candida albicans*.

- A New Modular Approach to Nanoassembly: Stable and Addressable DNA Nanoconstructs via Orthogonal Click Chemistries
  Gerrard, S. R.; Hardiman, C.; Shelbourne, M.; Nandhakumar, I.; Nordén, B.; Brown, T. *ACS Nano* **2012**, *6*, 9221-9228.
  Abstract:

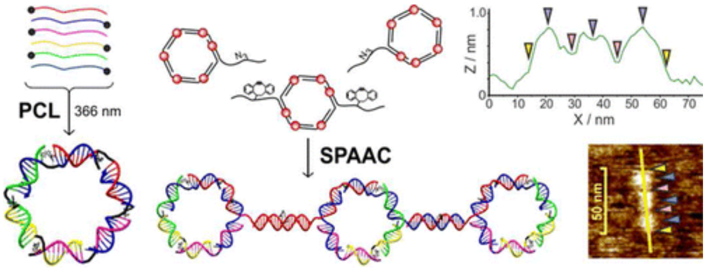

Thermodynamic instability is a problem when assembling and purifying complex DNA nanostructures formed by hybridization alone. To address this issue, we have used photochemical fixation and orthogonal copper-free, ring-strain-promoted, click chemistry for the synthesis of dimeric, trimeric, and oligomeric modular DNA scaffolds from cyclic, double-stranded, 80-mer DNA nanoconstructs. This particular combination of orthogonal click reactions was more effective for nanoassembly than others explored. The complex nanostructures are stable to heat and denaturation agents and can therefore be purified and characterized. They are addressable in a sequence-specific manner by triplex formation, and they can be reversibly and selectively deconstructed. Nanostructures utilizing this orthogonal, chemical fixation methodology can be used as building blocks for nanomachines and functional DNA nanoarchitectures.

- Molecular Mechanism of Surface-Assisted Epitaxial Self-Assembly of Amyloid-like Peptides
  Kang, S.; Li, H.; Huynh, T.; Zhang, F.; Xia, Z.; Zhang, Y.; Zhou, R. *ACS Nano* **2012**, *6*, 9276-9282.
  Abstract:

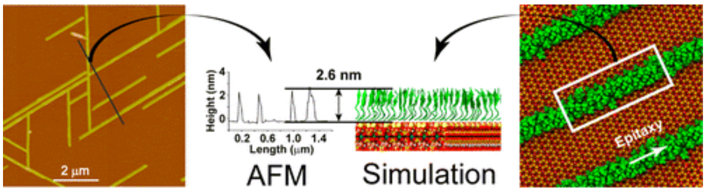

A surprising “upright” fibrilar conformation (with a height of ~2.6 nm) was observed with *in situ* atomic force microscopy (AFM) for an amyloid-like peptide (NH_2-VGGAVVAV-$COHN_2$) on mica surface, which is very different from its “flat” conformation (with a much smaller height of ~0.9 nm) on the HOPG surface. Our all-atom molecular dynamics (MD) simulations reveal that it is the strong electrostatic interactions between the N-terminus of the peptide and the mica surface that result in an upright conformation and a highly ordered β-stranded structure on mica, with a height of 2.5 ± 0.1 nm, consistent with the AFM experiment. Similarly, our MD simulations show that the same peptides adopt a flat conformation on HOPG surfaces due to the favorable hydrophobic interactions with

HOPG. Our simulations also indicate that epitaxial patterns found in mica are preferentially controlled by anisotropic binding sites commensurate with the inherent crystallographic unit cell of the basal substrate.

- Dynamic Nanoparticle Assemblies
  Wang, L.; Xu, L.; Kuang, H.; Xu, C.; Kotov, N. A. *Acc. Chem. Res.* **2012,** *45*, 1916-1926.
  Abstract:

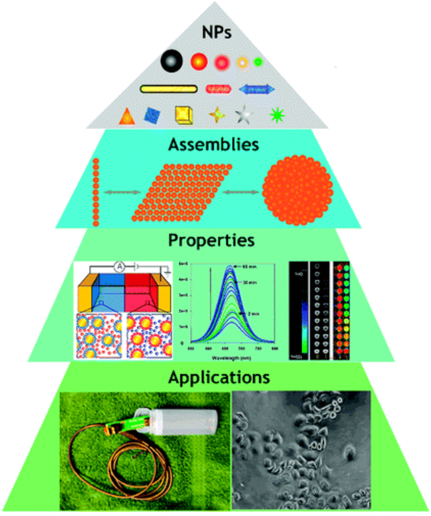

Although nanoparticle (NP) assemblies are at the beginning of their development, their unique geometrical shapes and media-responsive optical, electronic, and magnetic properties have attracted significant interest. Nanoscale assembly bridges multiple levels of hierarchy of materials: individual nanoparticles, discrete molecule-like or virus-like nanoscale agglomerates, microscale devices, and macroscale materials. The capacity to self-assemble can greatly facilitate the integration of nanotechnology with other technologies and, in particular, with microscale fabrication. In this Account, we describe developments in the emerging field of dynamic NP assemblies, which are spontaneously form superstructures containing more than two inorganic nanoscale particles that display the ability to change their geometrical, physical, chemical, and other attributes. In many ways, dynamic assemblies can represent a bottleneck in the "bottom-up" fabrication of NP-based devices because they can produce a much greater variety of assemblies, but they also provide a convenient tool for variation of geometries and dimensions of nanoparticle assemblies.

- Supra- and Nanocrystallinity: Specific Properties Related to Crystal Growth Mechanisms and Nanocrystallinity
  Pileni, M. P. *Acc. Chem. Res.* **2012,** *45*, 1965-1972.
  Abstract:

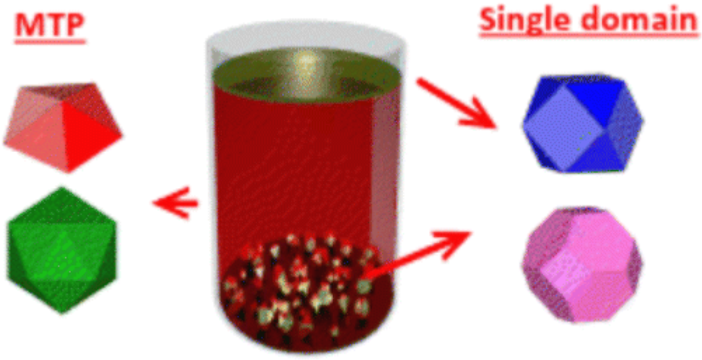

In this Account, we rationalize two simultaneous supracrystal growth processes that occur under saturated conditions, which form both well-defined 3D superlattices at the air–liquid interface and precipitated 3D assemblies with well-defined shapes. The growth processes of these colloidal crystals, called super- or supracrystals, markedly change the mechanical properties of these assemblies and induce the crystallinity segregation of nanocrystals. Therefore, single domain nanocrystals are the primary basis in the formation of these supracrystals, while multiply twinned particles (MTPs) and polycrystals remain dispersed within the colloidal suspension. Nanoindentation measurements show a drop in the Young's moduli for interfacial supracrystals in comparison with the precipitated supracrystals. In addition, the value of the Young's modulus changes markedly with the supracrystal growth mechanism. Using scanning tunneling microscopy/spectroscopy, we successfully imaged very thick supracrystals (from 200 nm up to a few micrometers) with remarkable conductance homogeneity and showed electronic fingerprints of isolated nanocrystals. This discovery of nanocrystal fingerprints within supracrystals could lead to promising applications in nanotechnology.

- Hopping transport and the Hall effect near the insulator–metal transition in electrochemically gated poly(3-hexylthiophene) transistors
  Wang, S.; Ha, M.; Manno, M.; Frisbie, C. D.; Leighton, C. *Nature Communications* **2012**, *3*, 1210.
  Abstract:

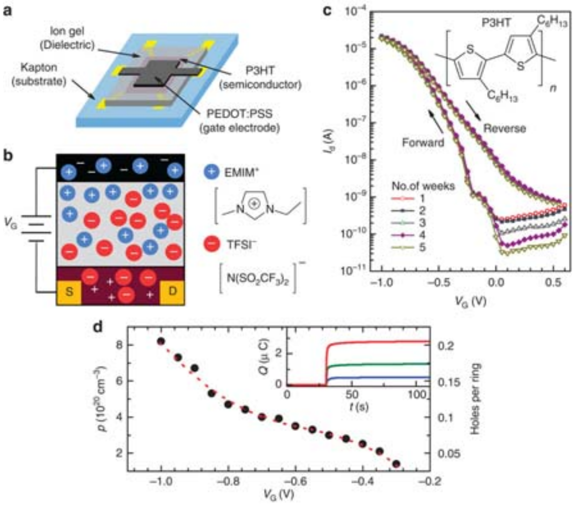

Despite 35 years of investigation, much remains to be understood regarding charge transport in semiconducting polymers, including the ultimate limits on their conductivity. Recently developed ion gel gating techniques provide a unique opportunity to study such issues at very high charge carrier density. Here we have probed the benchmark polymer semiconductor poly(3-hexylthiophene) at electrochemically induced three-dimensional hole densities approaching 10^{21} cm^{-3} (up to 0.2 holes per monomer). Analysis of the hopping conduction reveals a remarkable phenomenon where wavefunction delocalization and Coulomb gap collapse are disrupted by doping-induced disorder, suppressing the insulator–metal transition, even at these extreme charge densities. Nevertheless, at the highest dopings, we observe, for the first time in a polymer transistor, a clear Hall effect with the expected field, temperature and gate voltage dependencies. The data indicate that at such mobilities (~0.8 cm^{2}V^{-1} s^{-1}), despite the extensive disorder, these polymers lie close to a regime of truly diffusive band-like transport.

- Broadband electromagnetic cloaking with smart metamaterials
  Shin, D.; Urzhumov, Y.; Jung, Y.; Kang, G.; Baek, S.; Choi, M.; Park, H.; Kim, K.; Smith, D. R. *Nature Communications* **2012**, *3*, 1213.
  Abstract:

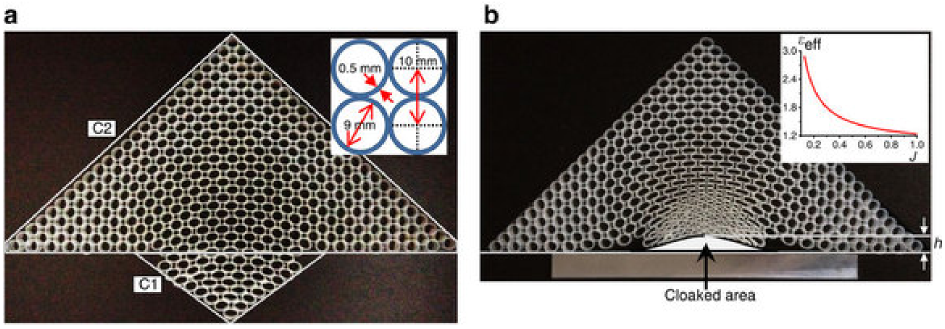

The ability to render objects invisible with a cloak that fits all objects and sizes is a long-standing goal for optical devices. Invisibility devices demonstrated so far typically comprise a rigid structure wrapped around an object to which it is fitted. Here we demonstrate smart metamaterial cloaking, wherein the metamaterial device not only transforms electromagnetic fields to make an object invisible, but also acquires its properties automatically from its own elastic deformation. The demonstrated device is a ground-plane microwave cloak composed of an elastic metamaterial with a broad operational band (10–12 GHz) and nearly lossless electromagnetic properties. The metamaterial is uniform, or perfectly periodic, in its undeformed state and acquires the necessary gradient-index profile, mimicking a quasi-conformal transformation, naturally from a boundary load. This easy-to-fabricate hybrid elasto-electromagnetic metamaterial opens the door to implementations of a variety of transformation optics devices based on quasi-conformal maps.

- Self-Assembly of Filamentous Amelogenin Requires Calcium and Phosphate: From Dimers via Nanoribbons to Fibrils
  Martinez-Avila, O.; Wu, S.; Kim, S. J.; Cheng, Y.; Khan, F.; Samudrala, R.; Sali, A.; Horst, J. A.; Habelitz, S. *Biomacromolecules* **2012**, *13*, 3494–3502.
  Abstract:

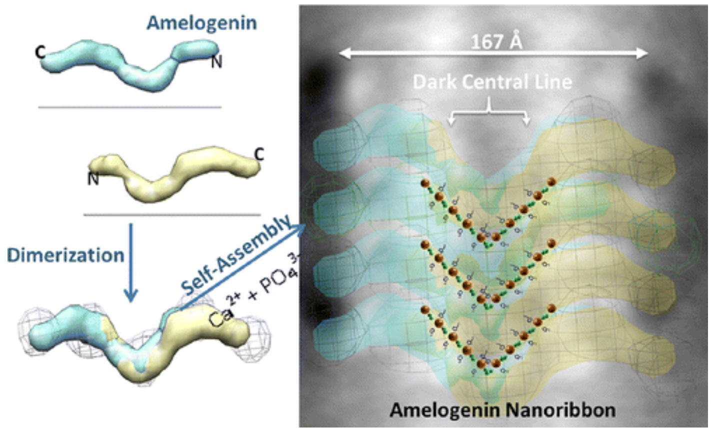

Enamel matrix self-assembly has long been suggested as the driving force behind aligned nanofibrous hydroxyapatite formation. We tested if amelogenin, the main enamel matrix protein, can self-assemble into ribbon-like structures in physiologic solutions. Ribbons 17 nm wide were observed to grow several micrometers in length, requiring calcium, phosphate, and pH 4.0–6.0. The pH range suggests that the formation of ion bridges through protonated histidine residues is essential to self-assembly, supported by a statistical analysis of 212 phosphate-binding proteins predicting 12

phosphate-binding histidines. Thermophoretic analysis verified the importance of calcium and phosphate in self-assembly. X-ray scattering characterized amelogenin dimers with dimensions fitting the cross-section of the amelogenin ribbon, leading to the hypothesis that antiparallel dimers are the building blocks of the ribbons. Over 5–7 days, ribbons self-organized into bundles composed of aligned ribbons mimicking the structure of enamel crystallites in enamel rods. These observations confirm reports of filamentous organic components in developing enamel and provide a new model for matrix-templated enamel mineralization.

- Formation of α-Helical Nanofibers by Mixing β-Structured and α-Helical Coiled Coil Peptides
  Brandenburg, E.; v. Berlepsch, H.; Leiterer, J.; Emmerling, F.; Koksch, B. *Biomacromolecules* **2012**, *13*, 3542–3551.
  Abstract:

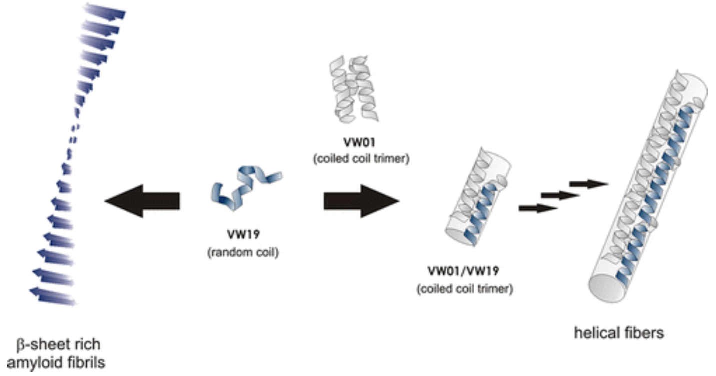

The helical coiled coil is a well-studied folding motif that can be used for the design of nanometer-sized bioinspired fibrous structures with potential applications as functional materials. A two-component system of coiled coil based model peptides is investigated, which forms, under acidic conditions, uniform, hundreds of nanometers long, and 2.6 nm thick trimeric α-helical fibers. In the absence of the other component and under the same solvent conditions, one model peptide forms β-sheet-rich amyloid fibrils and the other forms stable trimeric α-helical coiled coils, respectively. These observations reveal that the complementary interactions driving helical folding are much stronger here than those promoting the intermolecular β-sheet formation. The results of this study are important in the context of amyloid inhibition but also open up new avenues for the design of novel fibrous peptidic materials.

- Poly(vinyl alcohol) Hydrogel Can Autonomously Self-Heal
  Zhang, H.; Xia, H.; Zhao, Y. *ACS Macro Lett.* **2012**, *1*, 1233–1236.
  Abstract:

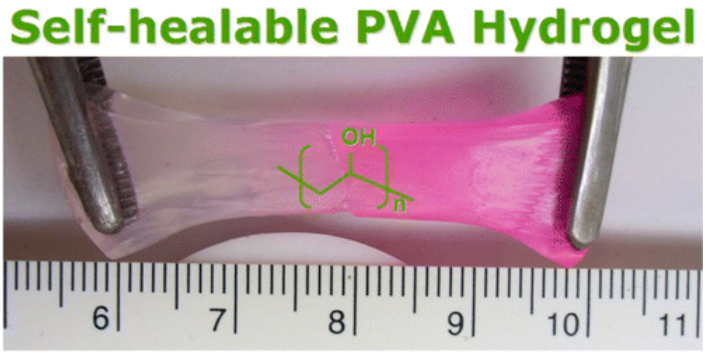

It is discovered that poly(vinyl alcohol) (PVA) hydrogel prepared using the freezing/thawing method can self-repair at room temperature without the need for any stimulus or healing agent. The autonomous self-healing process can be fast for mechanically strong PVA hydrogel yielding a high fracture stress. Investigation on the effect of the hydrogel preparation conditions points out that hydrogen bonding between PVA chains across the interface of the cut surfaces is at the origin of the phenomenon. The key for an effective self-healing is to have an appropriate balance between high concentration of free hydroxyl groups on PVA chains on the cut surfaces prior to contact and sufficient PVA chain mobility in the hydrogel.

- Multidimensional Assembly of S-Layer Proteins on Mobility-Controlled Polyelectrolyte Multilayers
  Ju Yeo, S.; Shin, S.-H.; Nam, K. T.; Yoo, P. J. *ACS Macro Lett.* **2012**, *1*, 1254–1257.
  Abstract:

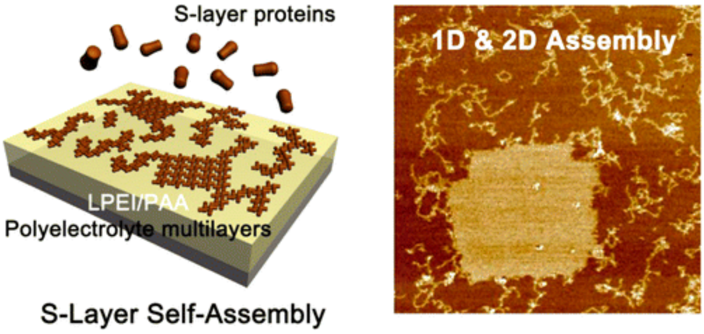

Polyelectrolyte multilayers have been vastly utilized as an assembling platform for various biomaterials because of their soft and charged surface characteristics, analogous to biomembrane systems. In particular, polyelectrolyte chains with high self-diffusivity can effectively transfer the surface mobility to the assembling biomolecular species, facilitating the ordered self-assembly. Herein, highly diffusional cationic polyelectrolyte chains of linear polyethylenimine are employed to induce direct binding with negatively charged bacterial surface layer proteins, which eventually lead to large-scale two-dimensional crystals. Notably, at the elevated incubation temperature, a transitory intermediate of one-dimensional chain structure is observed. We reveal that this one-dimensional intermediate is a stable precursor toward two-dimensional crystal arrays.

- Photoinduced Monolayer Patterning for the Creation of Complex Protein Patterns
  Hynes, M. J.; Maurer, J. A. *Langmuir* **2012**, *28*, 16237–16242.
  Abstract:

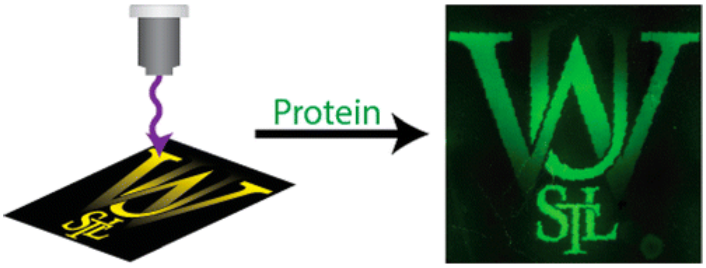

This work investigates self-assembled monolayers that were formed from a glycol-terminated thiol monomer and were patterned using photoinduced monolayer desorption. Utilizing direct-write photolithography provided a facile means to generate complex protein patterns containing gradients and punctate regions. The ablated glycol monolayers were characterized using scanning probe microscopy, which allowed us to observe differences in the nanomechanical properties between the patterned and nonpatterned regions of the substrate. The patterned regions on the surface adsorbed proteins, and this process was monitored quantitatively using surface plasmon resonance imaging (SPRi). Moreover, the concentration of the protein could be controlled accurately by simply setting the gray level in the 8-bit image. Adsorbed protein was probed using a commercially available antibody binding assay, which showed significant enhancement over the background. The ability to produce complex protein patterns will contribute greatly to creating in vitro models that more accurately mimic an in vivo environment.

- Preparation and Characterization of Conducting Mixed-Valence 9,9′-Dimethyl-3,3′-bicarbazyl Rectangular Nanowires
  Tokuda, T.; Murashiro, K.; Kubo, M.; Masu, H.; Imanari, M.; Seki, H.; Aoki, N.; Ochiai, Y.; Kanoh, H.; Hoshino, K. *Langmuir* **2012**, *28*, 16430–16435.
  Abstract:

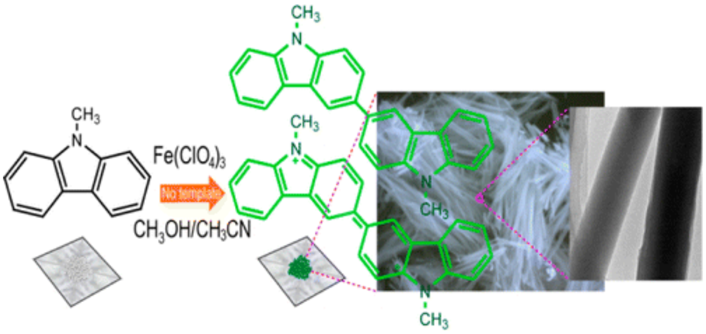

The facile synthesis of an organic electric conducting nanowire is described. The simple oxidation of 9-methylcarbazole by iron(III) perchlorate in a methanol/acetonitrile mixture under atmospheric pressure and temperature produces abundant nanowires without using a template. The nanowire consists of 9,9′-dimethyl-3,3′-dicarbazyl and has a rectangular nanowire shape with an average diameter of 397 ± 50 nm and length of 17 ± 5 µm. The results of the elemental analysis, ^{1}H NMR, FT-IR, XPS, and ESR measurements revealed that the chemical composition of the nanowire is $(\text{dicarbazyl})_{0.12}(\text{dicarbazylium}\cdot ClO_4^-)_{0.88}\cdot H_2O$. This result, combined with the UV–vis–NIR measurement, demonstrates that 9,9′-dimethyl-3,3′-dicarbazyl stacks in a mixed valence state. The nanowire is electroactive and has an electric conductivity of 3.0×10^{-5} S cm^{-1}.

- Thermo-responsive organic–inorganic hybrid vesicles with tunable membrane permeability
  Peng, B.; Liu, Y.; Shi, Y.; Li, Z.; Chen, Y. *Soft Matter* **2012**, *8*, 12002-12008.
  Abstract:

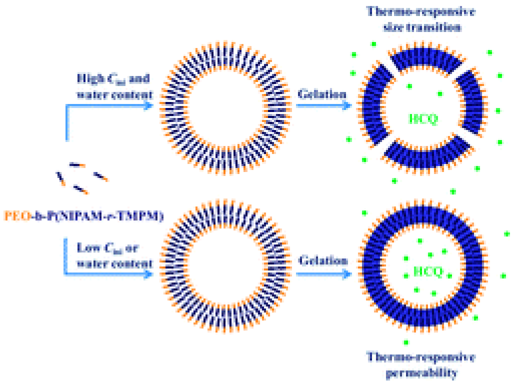

Herein, a series of crosslinked thermo-responsive organic–inorganic hybrid vesicles with different morphologies was prepared by the self-assembly of poly(ethylene oxide)-*block*-poly[*N*-isopropylacrylamide-*random*-3-(trimethoxysilyl)propyl methacrylate] [PEO-*b*-P(NIPAM-*r*-TMPM)] in DMF–water mixture. The copolymers were synthesized by reversible addition-fragmentation chain transfer (RAFT) mediated radical polymerization using a PEO macromolecular chain transfer agent. After self-assembly and gelation procedure in solution, porous vesicles and simple vesicles were obtained by tuning the solvent composition in the binary solvent mixture of water and DMF and the initial copolymer concentration (C_{ini}). The membranes of the as-formed vesicles were intact at C_{ini} = 10 mg mL^{-1}, 80 wt% H_2O, 28 °C; but, after gelation process, the pores of several tens of nanometers were generated within the membranes due to the crosslinking-induced tensile force. However, there was no morphology transition at low C_{ini} or low water content. The developments of vesicle size and the membrane permeability regarding change in temperature were studied by DLS analysis and Nile Red probe method. The cumulative release of a water-soluble model drug, hydroxychloroquine sulfate (HCQ), was used to determine the permeability of the gelated vesicles. While the gelated porous vesicles displayed no permeability dependence on temperature, the gelated simple vesicles exhibited enhanced permeability with temperature elevation. Also, with increase of the crosslinking density of membrane, numbers of TMPM units, the permeability of the simple vesicles was enhanced at 20 °C but remained unchanged at 45 °C.

- Solvent-chirality selective organogelation by chiral aspartame lipids
  Mukai, M.; Minamikawa, H.; Aoyagi, M.; Asakawa, M.; Shimizu, T.; Kogiso, M. *Soft Matter* **2012**, *8*, 11979-11981.
  Abstract:

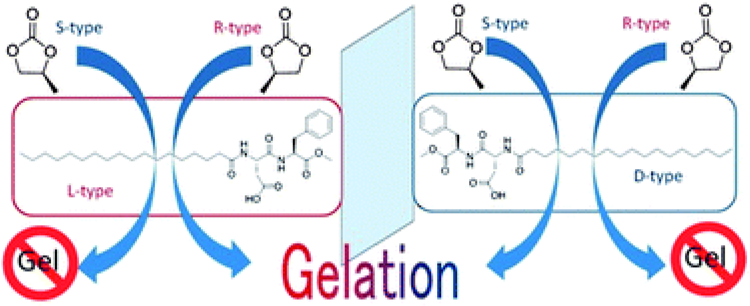

We examined supramolecular gelation of propylene carbonate enantiomers with novel chiral aspartame lipids. Different gelation ability and stability were observed based on the combination of gelator and the solvent enantiomers. This work demonstrates that gelator–solvent chirality matching can determine self-assembled nanostructures and gelation efficiency.

- Phenothiazine–triphenylamine based organic dyes containing various conjugated linkers for efficient dye-sensitized solar cells
  Wan, Z.; Jia, C.; Duan, Y.; Zhou, L.; Lin, Y.; Shi, Y. *J. Mater. Chem.* **2012**, *22*, 25140–25147.
  Abstract:

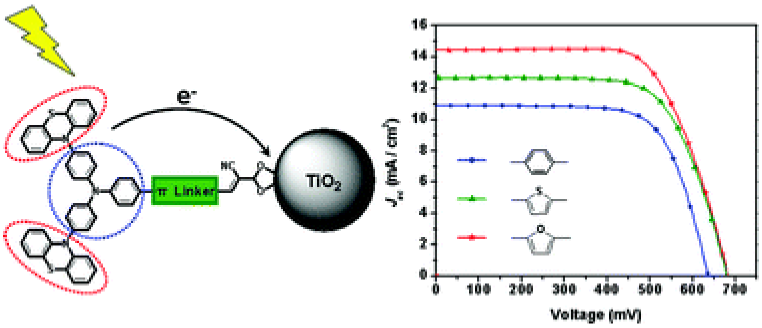

In order to increase the electron-donating ability of the donor part of the organic dye, two phenothiazine groups, as additional electron donors, were introduced into a triphenylamine unit to form a starburst donor–donor (2D) structure in this paper. Three new organic dyes (WD-6, WD-7 and WD-8) containing this starburst 2D structure and a 2-cyanoacetic acid acceptor linked by various conjugated linkers (benzene, thiophene, and furan) have been designed, synthesized and applied in dye-sensitized solar cells (DSSCs). The introduction of a phenothiazine group with a butterfly conformation in the triphenylamine donor parts has a good influence on preventing the molecular π–π aggregation due to the starburst 2D structure of the organic dye. The conjugated linker effects on the photophysical, electrochemical and photovoltaic properties of these organic dyes were investigated in detail. The DSSCs made with these organic dyes displayed remarkable overall conversion efficiencies, ranging from 4.90–6.79% under an AM 1.5 solar condition (100 mW cm^{-2}). The best performance was found for organic dye WD-8, in which a furan group was the conjugated linker. It displayed a short-circuit current (J_{sc}) of 14.43 mA cm^{-2}, an open-circuit voltage (V_{oc}) of 682 mV, and a fill factor (ff) of 0.69, corresponding to an overall conversion efficiency of 6.79%. The different photovoltaic behaviors of the solar cells based on these organic dyes were further elucidated by the electrochemical impedance spectroscopy.

- Artificial Muscles: A Tool To Quantify Exchanged Solvent during Biomimetic Reactions
  Otero, T. F.; Martinez, J. G.; Cheng, Y.-J.; Hsu, C.-S *Chem. Mater.* **2012**, *24*, 4093–4099.
  Abstract:

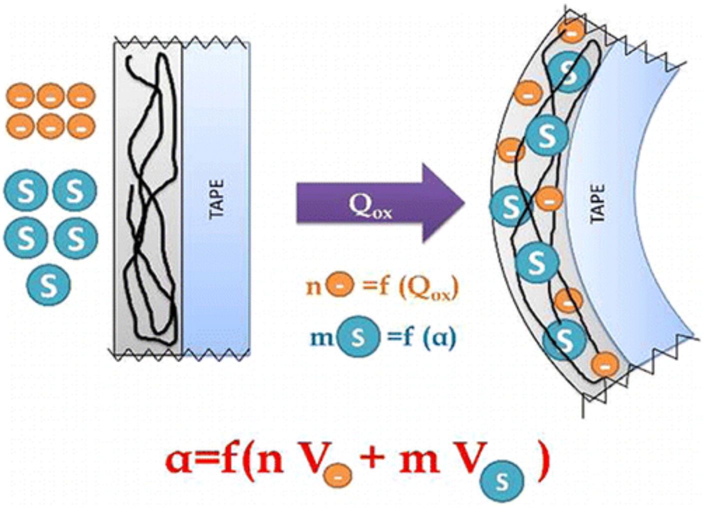

Artificial muscles (bending or linear) from films of conducting polymers are faradic and biomimetic gel motors consuming the same charge to move through the same space in a specific electrolyte. The driven volume variation of the film requires the exchange with the electrolyte of a number of counterions, defined by the charge, and solvent molecules during reactions. Working in aqueous solution with different anions using bilayer (polypyrrole/tape) bending artificial muscles, the charge consumed to describe a constant angle changes with the anion. Volume variations in the polypyrrole film due to the anionic exchange are calculated from the involved charge and the crystallographic radius of every anion. A parallel exchange of water molecules is required to explain the described angles. The number of solvent molecules exchanged between the polymeric membrane and the electrolyte at the same time that an anion (apparent solvation number) or when an electron was extracted from the chains (apparent hydration number) during the reaction was calculated. The use of artificial muscles (bending or linear) as a tool for the quantification of the number of solvent molecules accompanying the electrochemical reactions in p-doping or n-doping conducting polymers is proposed.